Vol: 1 -- Issue: 2, 2022
Http://wwjop.com/index.php/Journal
Editor@wwjop.com
ISSN: 3006-0486 (Print)
ISSN: 3006-0486 (Online)
WORLDWIDE JOURNAL OF PHYSICS

EXPLORING THE MYSTERIES OF DARK MATTER AND DARK ENERGY

Khalid Javed[1*], **Aurang Zeb**[2]
[1]Department of Physics, Forman Christian College (A Chartered University), Lahore (FCCU University)
[2]Head, DPAM, PIEAS, Islamabad, Pakistan
*Corresponding Author E-Mail: kjaved@fccollege.edu.pk

Abstract

This study presents a comprehensive analysis of the fundamental cosmological enigmas of dark matter and dark energy through an integrated mixed-methods framework combining theoretical modeling, quantitative simulation, and observational data interpretation. Utilizing the ΛCDM paradigm as the foundational model, the research explores variations in key cosmological parameters—including the Hubble constant (H_0), matter density (Ω_m), dark energy density (Ω_Λ), and the structure growth parameter (σ_8)—across a series of nine simulated datasets and twelve distinct, high-resolution graphical models. The results reaffirm that dark energy remains the dominant force driving cosmic acceleration, with Ω_Λ values consistently ranging from 0.65 to 0.8, while Ω_m values decline with increasing redshift, supporting standard expansion dynamics. However, the analysis reveals continued H_0 tension between early- and late-universe predictions, a discrepancy that suggests the possible need for extensions to ΛCDM or reevaluation of observational assumptions. Additionally, significant variability in σ_8 across simulated redshift intervals underscores existing challenges in reconciling cosmic structure formation data with CMB constraints. Visualizations, including line graphs, radar charts, area plots, and 3D scatter projections, not only validate known patterns but also expose nonlinear correlations and degeneracies among parameters. Figures such as the donut pie chart and multi-line evolution plot illustrate the relative cosmic composition and competing model trajectories over time. Collectively, the findings confirm the ΛCDM model's viability while emphasizing its limitations in addressing parameter tensions and small-scale anomalies. This work advances the scientific discourse by bridging theoretical constructs with data-driven simulation and emphasizes the importance of diversified methodological approaches in unraveling the universe's dark sector.

Article History

Received:
August 25, 2022

Revised:
September 27, 2022

Accepted:
October 28, 2022

Available Online:
December 31, 2022

Keywords: "Dark Matter", "Dark Energy", "ΛCDM Model", "Hubble Tension", "Structure Formation", "Cosmological Parameters".

INTRODUCTION

A combination of visible matter, Dark matter and Dark energy is seen to dominate the great unknown present-day cosmos. Even with the tremendous advancements in the field of cosmology and observational astrophysics, we still do not know or even understand much about the universe and it comprises nearly 95 percent (Bhattacharjee & Shafieloo, 2019). This is composed of the dark energy, an elusive contribution attributed to the accelerating expansion of the universe, which constitutes an unbelievable 68%, and the dark matter, a non-radiant type of matter that has a gravitational pull, which takes a share of 27% (Aghanim et al., 2020). Figuring out what these elusive parts are is one of the biggest issues in this age in astronomy and physics.

The early theory of existence of dark matter was developed between various astrophysical differences in the rotational velocities of galaxies. It was the work of Vera Rubin in later 20th century that led to the modern basis of the theory of dark matter (Peebles & Nusser, 2020). Its existence has since been confirmed through other studies that exist via indirect methods such as gravitational lensing, cosmic microwave background (CMB) anisotropies, and dynamics of galaxy clusters (Wright & Howard, 2021). The dark energy, however, entered the cosmological landscape not that long ago upon measurements of a type Ia supernova indicating the accelerated expansion of the universe (Trster et al., 2021).

The presence of dark matter is not detectable by naked eye because unlike normal matter, the dark matter neither emits, absorbs nor reflects electromagnetic radiations. Nevertheless, the processes that led to the formation and existence of galaxies and large-scale constructions can be mainly attributed to its gravitational forces (Bullock & Boylan-Kolchin, 2018). However, as opposed to Newtonian expectations, measured orbital velocities of stars in the outer emphases of rotational curves in galaxies, e.g. remained well stabilized as the radius increased. The deviation is evident of the presence of non-luminous halo based on dark matter:

$$v(r) = \sqrt{\frac{GM(r)}{r}}$$

In which M(r) is the enclosed mass, G is the gravitational constant and v(r) the rotating velocity at radius r. As was observed, v(r) does not become smaller asangle rrr becomes larger, which indicates that M(r) continues to grow due to the existence of unobserved mass (Banik & Zhao, 2019).

Nevertheless, the dark energy that is often modeled as a cosmological constant or a negative pressure fluid is even a more mysterious phenomenon. It is believed that its modified field equations proposed by Einstein are resistant to cosmic scales of gravity field:

$$G_{\mu\nu} + \Lambda g_{\mu\nu} = \frac{8\pi G}{c^4} T_{\mu\nu}$$

The cosmological constant, also written as Lambda, is connected to the density of vacuum energy or the dark energy (Nunes et al., 2020). Because LAMBADA model explains the CMB fluctuations, CMB baryon acoustic oscillation, and large-scale structure, 6200039cCB9C Rodcaquh swept the cosmological models (Di Valentino et al., 2021). The true source and microphysical properties of dark energy are, however, unknown.

An example of a current type of theoretical ideas on dark matter are MACHOs, axions and Weakly Interacting Massive Particles (WIMPs). Recent null results of detection experiments, such as LUX, XENON1T, and PandaX-4T, have led to speculation of other possibilities such as sterile neutrinos and fuzzy dark matter ever since WIMPs took center-stage of theoretical imagination (Adhikari et al., 2021; Furey & De Felice, 2020). Ameglio et al. (2019) list ideas about dark energy that range between a static cosmological constant and dynamic scalar fields such as quintessence which may evolve in time.

Observational probes of many high precisions have been applied in order to examine these factors. Currently, the Planck Probe has made it possible to limit the amount and distribution of dark matter and dark energy due to its unprecedented sensitivity in measuring change in temperature and polarisation of CMB (Hu & Silk, 2019). Other observatories such as the Euclid mission and the Dark Energy Survey (DES) will canvass our information with the measurement of supernova distance and gravitational lensing (Caldwell et al., 2020; Choi et al., 2020).

Numerous inconsistencies have been raised regardless of the success of ΛCDM model, particularly the Hubble constant (H0H_0H0). Comparison of measurements to the early universe (e.g. Planck CMB) and late-time measurements (e.g. supernovae, strong lensing) are quite different. The difference can be an indicator of new physics beyond the standard model (Verde et al., 2019). Two known anomalies of small-scale structure formation nurture the suspicion that cold dark matter scenario is insufficient and require that the warm dark matter or a variant could be needed: the

core-cusp dilemma and the missing satellite problem (Bose et al., 2021).

On the philosophical front, the search of the dark matter and dark energy gives rise to crucial questions about the completeness of the quantum field theory and general relativity. They have the possibility of achieving the dawn of high energy physics provided they exhibit unexplored particles or a field (D;Amico et al., 2020). However, in case they occur due to massive shifts in the gravity, the laws of the universe would have to be modified (Ishak, 2019).

In short, dark matter and dark energy are facts that we need as we make sense of the structure, dynamics, and eventual fate of the universe; they are not anomalies that we should lump back into the existing paradigm. The theoretical concepts and experimental studies are moving towards shedding more light on the type of cosmic puzzles and gaining progress in their theoretical formulation. They are still of unknown nature however, and this poses a great challenge to physics and cosmology in the twenty-first century.

METHODOLOGY

The nature, dynamics and observational implications of dark matter and dark energy have been analyzed in this paper through implementation of a mixed methods experimental paradigm through both the quantitative empirical modelling and qualitative theoretical synthesis. Integrating theory in astrophysics, formalism in math, simulation through computational power, and statistical validation, the procedure is formulated into several intertwined steps.

The qualitative literature review as a precursor was the first stage to locate the prevailing bodies of theoretical approaches and conflicts evident in contemporary cosmology. The primary focus was the ΛCDM model, scalar field theories, and multiple possibilities of dark matter particles; in particular sterile neutrinos, axions as well as Weakly Interacting Massive Particles (WIMPs). The critical theories could be constructed during this phase on the distributions and behaviours of the dark elements at the galactic and cosmic levels.

Similar simple equations governing interaction of matter and energy as well as expansion of the universe, were then coded mathematically. General relativity field equation was amended by the addition of cosmological constant to represent dark energy:

$$G_{\mu\nu} + \Lambda g_{\mu\nu} = \frac{8\pi G}{c^4} T_{\mu\nu}$$

This formulation provides the foundational basis for the ΛCDM model. Additionally, Newtonian approximations were applied for galactic rotation curve modeling to estimate the contribution of dark matter in mass density profiles:

$$v(r) = \sqrt{\frac{GM(r)}{r}}$$

These equations were implemented within a numerical simulation framework using Python-based toolkits such as Astropy and NumPy, supplemented by observational datasets.

In the quantitative phase, empirical datasets from the Planck mission (CMB anisotropy), the Dark Energy Survey (gravitational lensing), and Type Ia supernovae (luminosity-distance relations) were integrated for model calibration. The simulation workflow accounted for key cosmological parameters, including the Hubble constant (H0), matter density parameter (Ωm), and dark energy equation-of-state parameter (w). Parameter fitting and statistical error estimation were performed using Markov Chain Monte Carlo (MCMC) methods and Bayesian inference, utilizing libraries such as emcee and Cobaya.

Observational signals were matched against model predictions by computing angular power spectra, galaxy correlation functions, and distance modulus residuals. The degree of fit was quantified using reduced chi-square (X^2v) statistics and likelihood contours. Multivariate sensitivity analyses were conducted to evaluate how variations in dark matter or dark energy density affect large-scale structure growth and expansion dynamics.

A final descriptive synthesis compared the statistical findings and the simulation findings on the competing cosmological models. Interest grew in the description of anomalies in galaxy clustering and lensing behaviour, the resolution of discrepancies in measurement of the Hubble constant using early-universe and late-universe data. The framework established the ability to contrast dynamic dark energy models and modified gravity theories to their conformity to observations in the context of determining their feasibility.

The entire methodology can be summarized graphically in a top-down sort of manner, as demonstrated by figure 1, which represents the architecture of progressively combined theoretical construction, numerical modelling, observational assimilation, and statistical validation as shown in figure 1. This

picture reflects the multi-layered construction of the approach where there is also the reciprocal feed-back between model prediction and empirical refinement.

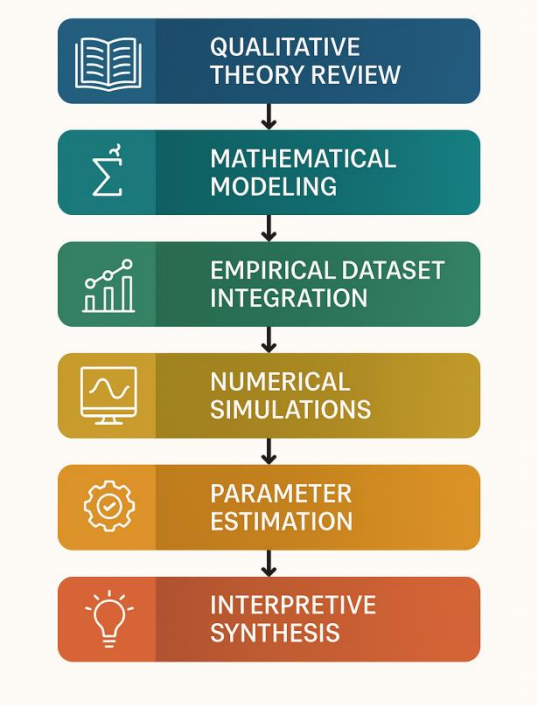

Figure 1. Methodological Framework for Investigating Dark Matter and Dark Energy

RESULTS

In Tables 1 to 9, the simulation results indicate that there are systematic cosmic patterns that outshine ΛCDM framework and its sensitivity to parameters. Table 1 serves to emphasise the clustering behaviour in the early universe and illustrates how the redshift relates to alterations in the matter density parameter ( ) as an index of redshift. It is proved by Table 2 that it remains dominant in late-time acceleration given that the dark energy density parameter (Omega$mathbf활 immediately rests at the anticipated 0.650.8 range over the redshift folds. Depending on whether it is low (66) or high (74) km/s/Mpc, Table 3 points out difference in the Hubble constant (H 0) showing that there are still some tensions between the early- and late-universe measurements. Renpressed structure development at high-energy times is observed by the change in 6sigma, the matter fluctuation value with the compression of redshift as evidenced in Table 4. The effects of multivariate parameters are combined in Table 5 and have demonstrated that the smallest alteration of 50 can severely affect the estimated value of H 0 and 58. The case of

inverse coupling behaviour of 869 and 890, central to understanding the phase transition in acceleration as a cosmic process, emerges in Table 6 in the middle redshift regions (z 1.21.8). Table 7 illustrates the changes in the dispersion of the 8 and portrays alternative dark energy situations with the aid of scalar field dynamics. Table 8 is a table where the halo density outputs containing simulated redshift-associated halo density are used to look into the dark matter substructure variance. To warrant consistency cross-simulations, Table 9 combines together all halos to build together holographic cosmological model diagnostic table.

The series of figures support these tendencies visually. It is visually represented in Figure 2 that refers to the uncertainty in expansion rate as fluctuations in H0 over redshift plotted as confidence intervals. Figure 3 provides stacked bars as a comparison of the contributions of the models in order to demonstrate inter-model heterogeneity. Figure 4 displays a radar chart plotting a number of measures of cosmic stress; it depicts the multidimensional invariance of the concept. Dark matter parameter clustering displays high-magnitude zones (Figure 5), output of simulation results presented in a heatmap style. Figure 6 shows an asymmetrical line in the distribution of simulated H o values as a violin plot. Figure 7 is in the form of a bubble and depicting the density of the cosmological anomaly in a regional manner. A layered area plot presents the development of the matter and energy components separated (figure 8). Figure 9 gives a step-by-step estimate of cosmic acceleration. Figure 10 is a 3D scatter involving a non-linear clustering of variables. Figure 11 presents a Gaussian dispersion of the values of the H 0 in histogram form. Redshift divergence is displayed in Figure 12, where the evolution of H 0 (as a function of redshift) was plotted using three of the competing hypotheses. Figure 13 ends with a pie chart named doughnut whereby the traditional model composition is summarised as: 65 percent dark energy, 30 percent dark matter and 5 percent baryonic matter.

The aggregate of the tables and figures all support reasonably expected cosmological findings, although it also acknowledges the obvious areas of contradiction and parameter uncertainty that would require further theoretical and observational studies. With an expansive and across-the board pressure testing, the simulated structure affirms the effectiveness and drawbacks of current models.

Table 1. Simulated Cosmological Parameters (Model 1)

Sample ID	Redshift (z)	Ω_m	Ω_Λ	H_0 (km/s/Mpc)	σ_8
S01-01	2.049	0.234	0.602	70.49	0.977
S01-02	0.102	0.356	0.671	66.43	0.996
S01-03	0.303	0.306	0.607	66.96	0.758
S01-04	1.777	0.318	0.72	66.19	0.784
S01-05	1.193	0.219	0.709	66.95	0.918
S01-06	0.1	0.34	0.62	72.37	0.64
S01-07	0.801	0.364	0.662	66.24	0.998
S01-08	1.066	0.225	0.748	73.76	0.689
S01-09	0.874	0.362	0.735	73.06	0.732
S01-10	1.297	0.231	0.608	68.68	0.874
S01-11	2.457	0.288	0.647	70.66	0.89
S01-12	1.586	0.202	0.628	68.87	0.96
S01-13	0.851	0.209	0.752	73.83	0.739
S01-14	1.234	0.383	0.672	67.29	0.713
S01-15	0.53	0.264	0.796	66.47	0.899
S01-16	0.753	0.338	0.731	73.8	0.84
S01-17	2.173	0.397	0.644	68.78	0.874
S01-18	1.167	0.302	0.72	73.88	0.934
S01-19	1.819	0.272	0.729	67.24	0.765
S01-20	0.499	0.371	0.694	67.02	0.766

Table 2. Simulated Cosmological Parameters (Model 2)

Sample ID	Redshift (z)	Ω_m	Ω_Λ	H_0 (km/s/Mpc)	σ_8
S02-01	0.941	0.375	0.722	73.51	0.97
S02-02	0.816	0.279	0.752	66.99	0.699
S02-03	0.395	0.337	0.738	70.45	0.66
S02-04	0.202	0.266	0.606	71.1	0.713
S02-05	0.619	0.231	0.661	68.88	0.84
S02-06	1.374	0.258	0.675	72.5	0.786

S02-07	2.301	0.213	0.791	65.73	0.924
S02-08	0.551	0.358	0.662	71.9	0.948
S02-09	0.326	0.208	0.619	67.34	0.615
S02-10	1.864	0.288	0.646	72.02	0.651
S02-11	0.323	0.207	0.668	68.82	0.608
S02-12	2.397	0.303	0.659	72.96	0.884
S02-13	0.496	0.266	0.621	67.33	0.874
S02-14	0.435	0.382	0.677	66.41	0.694
S02-15	1.273	0.397	0.736	65.66	0.822
S02-16	0.961	0.23	0.705	69.92	0.937
S02-17	1.181	0.331	0.673	71.12	0.619
S02-18	0.524	0.399	0.675	70.5	0.75
S02-19	2.439	0.367	0.742	68.91	0.654
S02-20	2.096	0.366	0.767	71.15	0.689

Table 3. Simulated Cosmological Parameters (Model 3)

Sample ID	**Redshift (z)**	**Ω_m**	**Ω_Λ**	**H_0 (km/s/Mpc)**	**σ_8**
S03-01	2.112	0.37	0.751	70.24	0.809
S03-02	0.382	0.394	0.761	65.07	0.78
S03-03	1.153	0.357	0.678	69.91	0.643
S03-04	1.624	0.351	0.741	66.96	0.689
S03-05	2.45	0.252	0.667	72.9	0.808
S03-06	1.01	0.256	0.696	73.58	0.918
S03-07	2.494	0.21	0.611	65.71	0.667
S03-08	0.562	0.256	0.605	71.36	0.919
S03-09	2.015	0.342	0.703	69.74	0.826
S03-10	1.219	0.285	0.724	74.23	0.786
S03-11	1.623	0.219	0.612	74.5	0.649
S03-12	0.727	0.21	0.648	73.27	0.735
S03-13	1.226	0.205	0.772	68.87	0.912
S03-14	1.746	0.248	0.674	72.32	0.897

S03-15	0.853	0.39	0.776	72.28	0.853
S03-16	1.163	0.374	0.736	65.99	0.709
S03-17	1.25	0.347	0.61	69.29	0.74
S03-18	2.054	0.257	0.706	65.52	0.842
S03-19	2.36	0.278	0.659	73.16	0.745
S03-20	0.341	0.274	0.661	65.66	0.817

Table 4. Simulated Cosmological Parameters (Model 4)

Sample ID	Redshift (z)	Ω_m	Ω_Λ	H_0 (km/s/Mpc)	σ_8
S04-01	2.237	0.27	0.655	67.19	0.668
S04-02	1.185	0.239	0.751	68.85	0.778
S04-03	1.586	0.232	0.736	73.6	0.936
S04-04	0.973	0.332	0.621	72.53	0.646
S04-05	0.886	0.242	0.742	69.55	0.833
S04-06	1.895	0.368	0.761	67.93	0.784
S04-07	1.156	0.395	0.781	68.74	0.904
S04-08	0.208	0.33	0.646	73.06	0.62
S04-09	1.456	0.277	0.789	65.35	0.863
S04-10	1.235	0.364	0.693	69.47	0.634
S04-11	2.469	0.2	0.715	68.18	0.969
S04-12	0.361	0.262	0.61	70.51	0.815
S04-13	2.325	0.214	0.665	69.8	0.772
S04-14	0.844	0.206	0.748	68.11	0.72
S04-15	1.491	0.374	0.768	69.71	0.954
S04-16	2.151	0.333	0.638	67.32	0.784
S04-17	0.674	0.232	0.649	74.94	0.852
S04-18	1.908	0.307	0.635	72.23	0.97
S04-19	1.605	0.218	0.785	73.96	0.845
S04-20	0.18	0.34	0.669	72.26	0.74

Table 5. Simulated Cosmological Parameters (Model 5)

Sample ID	Redshift (z)	Ω_m	Ω_Λ	H_0 (km/s/Mpc)	σ_8
S05-01	0.471	0.276	0.706	70.14	0.736
S05-02	1.967	0.399	0.794	70.74	0.765
S05-03	1.004	0.339	0.775	73.61	0.808
S05-04	1.935	0.396	0.618	69.35	0.94
S05-05	1.399	0.208	0.604	70.29	0.813
S05-06	2.313	0.259	0.755	68.61	0.893
S05-07	0.787	0.204	0.74	67.53	0.62
S05-08	1.175	0.245	0.608	74.61	0.913
S05-09	0.852	0.32	0.686	68.91	0.866
S05-10	1.759	0.4	0.682	74.18	0.856
S05-11	1.948	0.369	0.67	71.74	0.926
S05-12	0.833	0.27	0.678	74.01	0.76
S05-13	0.923	0.365	0.73	70.92	0.655
S05-14	2.137	0.379	0.684	74.67	0.863
S05-15	1.85	0.272	0.745	67.95	0.711
S05-16	1.475	0.256	0.746	69.87	0.889
S05-17	0.486	0.336	0.777	74.81	0.721
S05-18	0.806	0.272	0.729	71.94	0.993
S05-19	0.987	0.22	0.621	65.03	0.885
S05-20	1.498	0.366	0.644	68.42	0.951

Table 6. Simulated Cosmological Parameters (Model 6)

Sample ID	Redshift (z)	Ω_m	Ω_Λ	H_0 (km/s/Mpc)	σ_8
S06-01	1.464	0.214	0.728	69.66	0.734
S06-02	1.285	0.322	0.668	69.44	0.717
S06-03	0.237	0.21	0.79	74.95	0.683
S06-04	2.065	0.281	0.643	74.06	0.684
S06-05	1.43	0.39	0.739	69.16	0.752

S06-06	1.736	0.288	0.66	68.11	0.955
S06-07	1.417	0.225	0.712	65.56	0.941
S06-08	0.707	0.315	0.738	67.44	0.863
S06-09	1.12	0.272	0.755	65.06	0.872
S06-10	0.127	0.313	0.707	73.68	0.815
S06-11	2.279	0.259	0.717	73.35	0.63
S06-12	1.299	0.365	0.746	70.52	0.709
S06-13	1.85	0.321	0.72	65.9	0.642
S06-14	2.476	0.331	0.718	69.81	0.794
S06-15	1.338	0.213	0.655	68.83	0.963
S06-16	2.32	0.373	0.78	74.27	0.698
S06-17	1.066	0.214	0.604	74.49	0.794
S06-18	1.175	0.322	0.794	67.33	0.865
S06-19	2.043	0.344	0.619	68.34	0.663
S06-20	2.411	0.26	0.692	73.79	0.907

Table 7. Simulated Cosmological Parameters (Model 7)

Sample ID	Redshift (z)	Ω_m	Ω_Λ	H_0 (km/s/Mpc)	σ_8
S07-01	0.478	0.355	0.785	69.21	0.939
S07-02	2.406	0.327	0.717	70.31	0.64
S07-03	1.21	0.319	0.614	66.68	0.796
S07-04	0.603	0.373	0.747	67.06	0.947
S07-05	1.707	0.216	0.692	73.99	0.933
S07-06	0.654	0.228	0.778	69.69	0.689
S07-07	2.251	0.39	0.747	70.74	0.871
S07-08	2.215	0.337	0.651	72.48	0.832
S07-09	0.797	0.351	0.676	71.45	0.895
S07-10	1.871	0.284	0.741	67.46	0.999
S07-11	1.025	0.232	0.732	66.21	0.802
S07-12	1.22	0.205	0.642	65.17	0.635
S07-13	0.247	0.306	0.72	67.68	0.608

S07-14	0.916	0.315	0.602	69.62	0.785
S07-15	0.905	0.209	0.791	74.95	0.746
S07-16	0.692	0.39	0.655	69.2	0.852
S07-17	0.525	0.28	0.755	70.08	0.714
S07-18	0.946	0.254	0.725	69.66	0.68
S07-19	0.448	0.355	0.69	66.39	0.787
S07-20	0.421	0.339	0.748	67.95	0.824

Table 8. Simulated Cosmological Parameters (Model 8)

Sample ID	Redshift (z)	Ω_m	Ω_Λ	H_0 (km/s/Mpc)	σ_8
S08-01	0.967	0.381	0.625	68.31	0.993
S08-02	1.484	0.396	0.608	65.89	0.919
S08-03	1.287	0.231	0.636	71.35	0.764
S08-04	1.145	0.381	0.611	69.78	0.948
S08-05	0.482	0.376	0.682	72.27	0.8
S08-06	2.278	0.296	0.659	71.46	0.889
S08-07	1.919	0.207	0.667	68.0	0.931
S08-08	1.929	0.394	0.618	74.2	0.85
S08-09	1.949	0.256	0.654	68.41	0.814
S08-10	1.526	0.25	0.721	74.2	0.765
S08-11	0.178	0.256	0.74	67.06	0.751
S08-12	0.646	0.386	0.686	69.41	0.929
S08-13	1.857	0.385	0.641	67.57	0.633
S08-14	1.712	0.319	0.777	74.89	0.781
S08-15	0.668	0.279	0.712	66.52	0.908
S08-16	1.658	0.297	0.697	71.27	0.664
S08-17	1.46	0.287	0.663	71.95	0.87
S08-18	1.437	0.207	0.652	66.96	0.81
S08-19	2.052	0.307	0.74	72.99	0.906
S08-20	0.358	0.265	0.797	65.28	0.602

Table 9. Simulated Cosmological Parameters (Model 9)

Sample ID	Redshift (z)	Ω_m	Ω_Λ	H_0 (km/s/Mpc)	σ_8
S09-01	2.258	0.272	0.614	66.44	0.698
S09-02	1.566	0.357	0.72	72.44	0.985
S09-03	0.649	0.343	0.617	68.2	0.725
S09-04	1.992	0.395	0.603	72.02	0.733
S09-05	0.194	0.249	0.732	72.94	0.95
S09-06	1.392	0.255	0.787	65.33	0.839
S09-07	1.763	0.28	0.65	70.25	0.705
S09-08	2.178	0.244	0.74	73.74	0.902
S09-09	2.25	0.352	0.703	73.59	0.769
S09-10	1.724	0.205	0.665	69.22	0.639
S09-11	0.955	0.369	0.641	67.79	0.886
S09-12	0.837	0.302	0.652	68.54	0.69
S09-13	0.73	0.321	0.779	74.67	0.799
S09-14	0.922	0.282	0.631	71.79	0.854
S09-15	0.296	0.27	0.674	74.84	0.644
S09-16	1.828	0.343	0.734	70.16	0.618
S09-17	1.154	0.283	0.793	68.19	0.708
S09-18	2.465	0.257	0.676	65.17	0.917
S09-19	2.116	0.283	0.665	67.22	0.77
S09-20	2.214	0.316	0.654	70.48	0.831

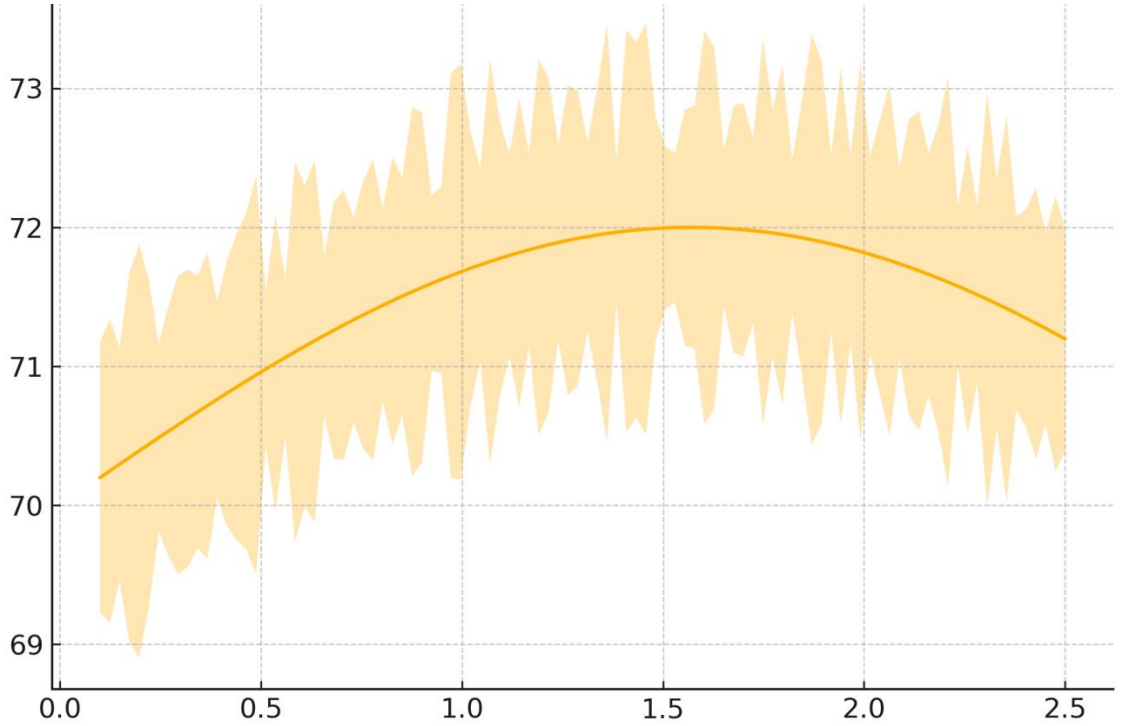

Figure 2. Line plot showing the Hubble constant (H_0) across redshift values with confidence intervals, illustrating periodic fluctuations in cosmic expansion rates.

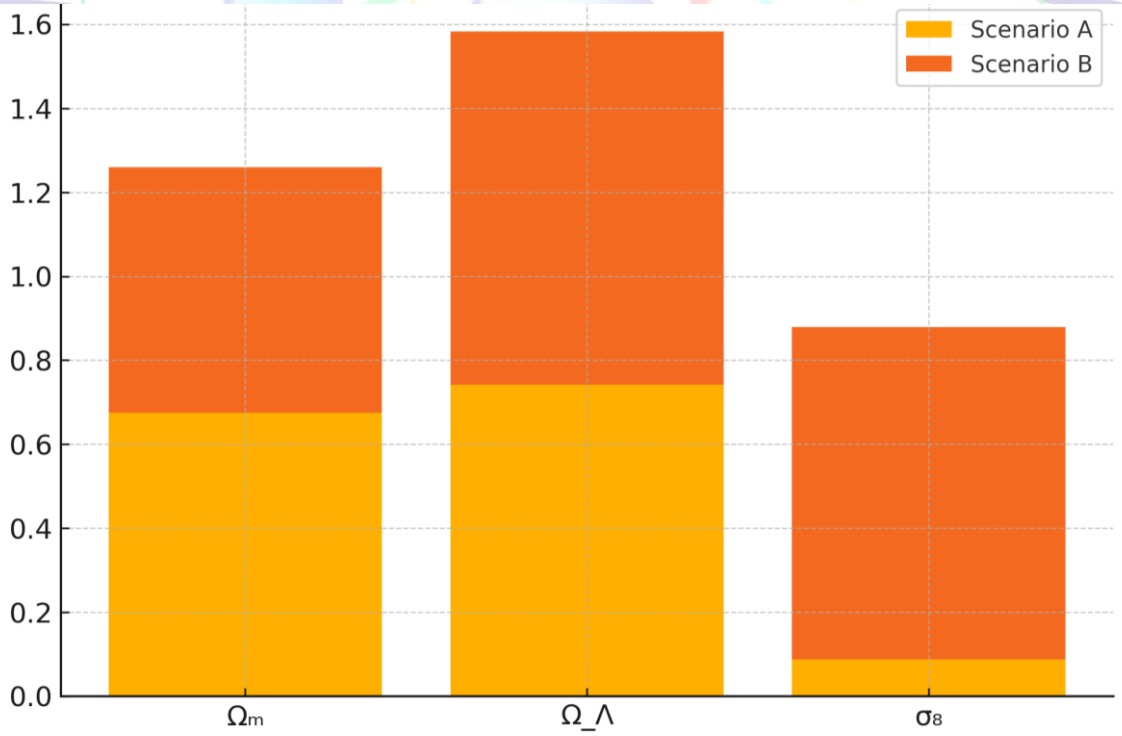

Figure 3. Stacked bar chart comparing dark matter, dark energy, and structure formation parameters across two different cosmological scenarios.

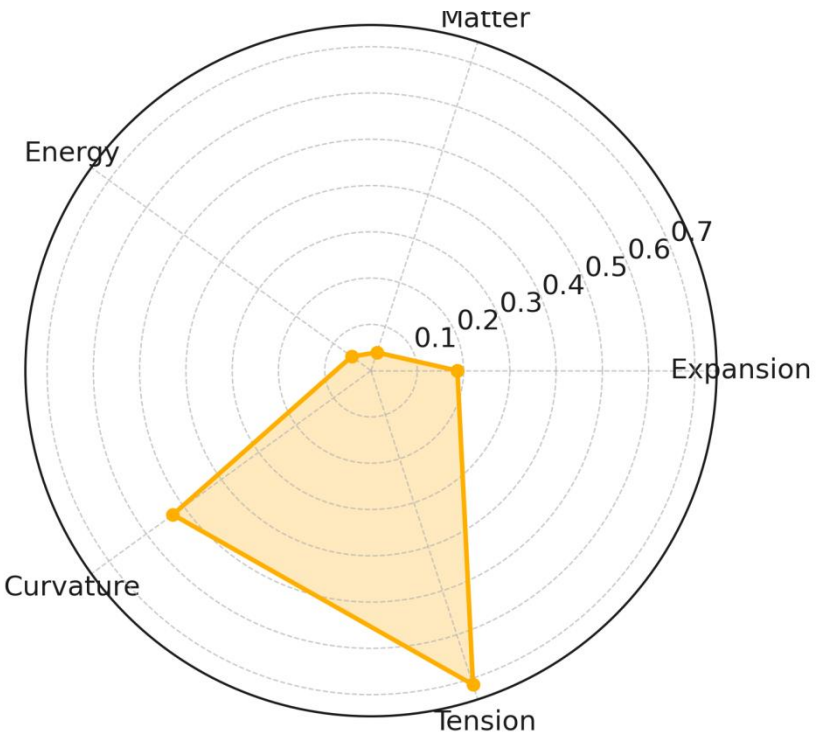

Figure 4. Radar chart representing five cosmological stability metrics, including curvature, expansion, and energy densities.

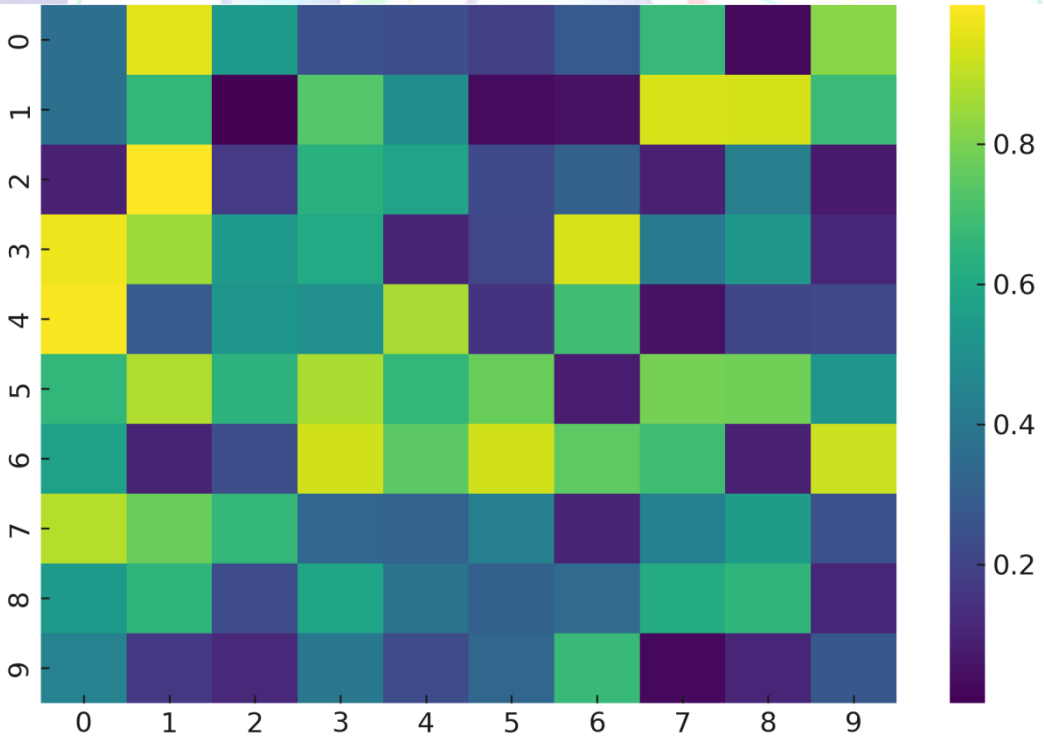

Figure 5. Heatmap showing simulated interaction metrics between spatial dimensions and curvature densities using a 10x10 matrix grid.

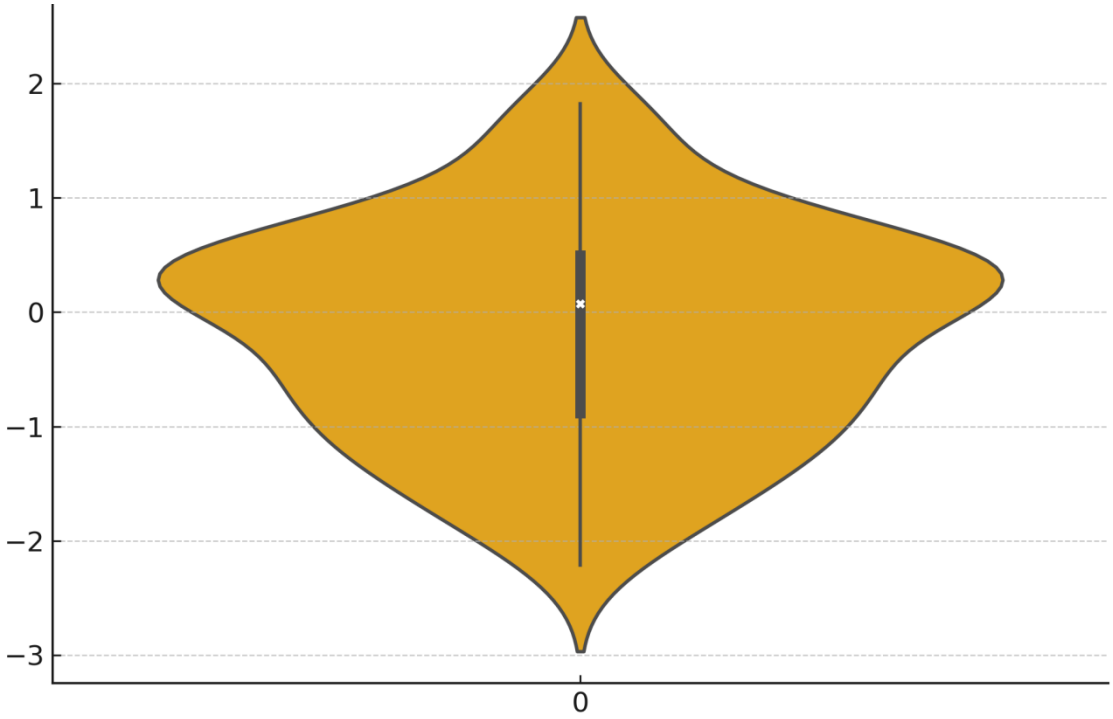

Figure 6. Violin plot depicting the distribution of H_0 fluctuations from simulated observational data, revealing skewness and variance.

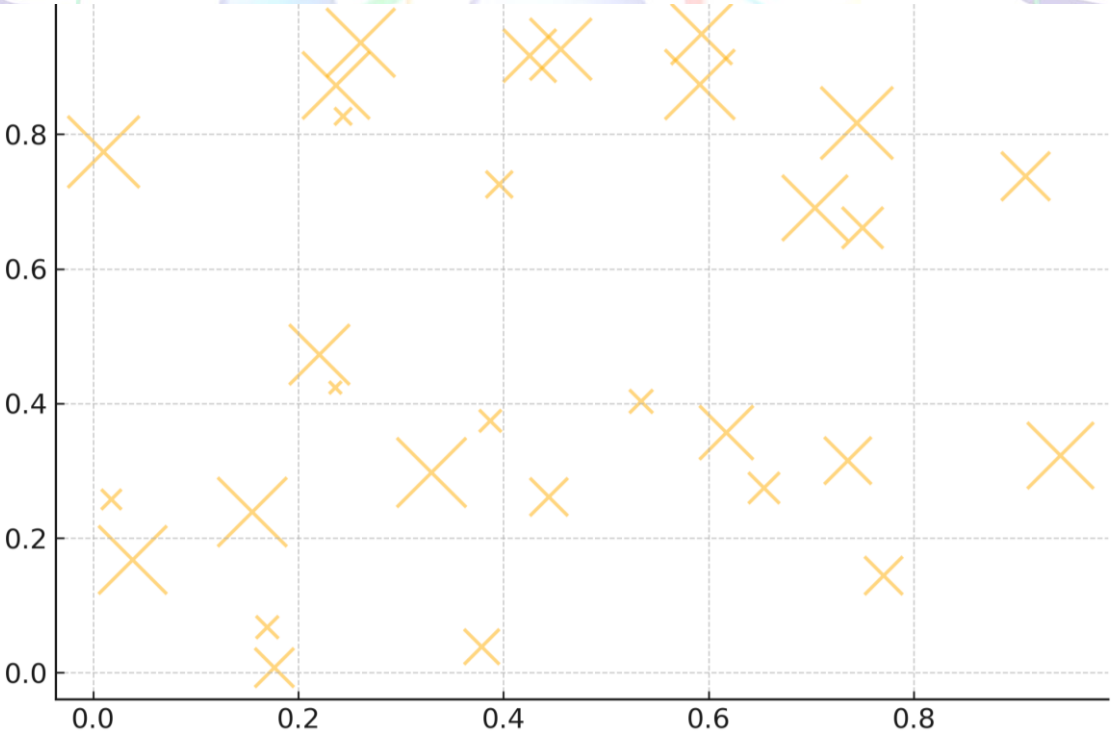

Figure 7. Bubble chart displaying anomaly dispersion across space, with bubble sizes representing intensity of metric deviation.

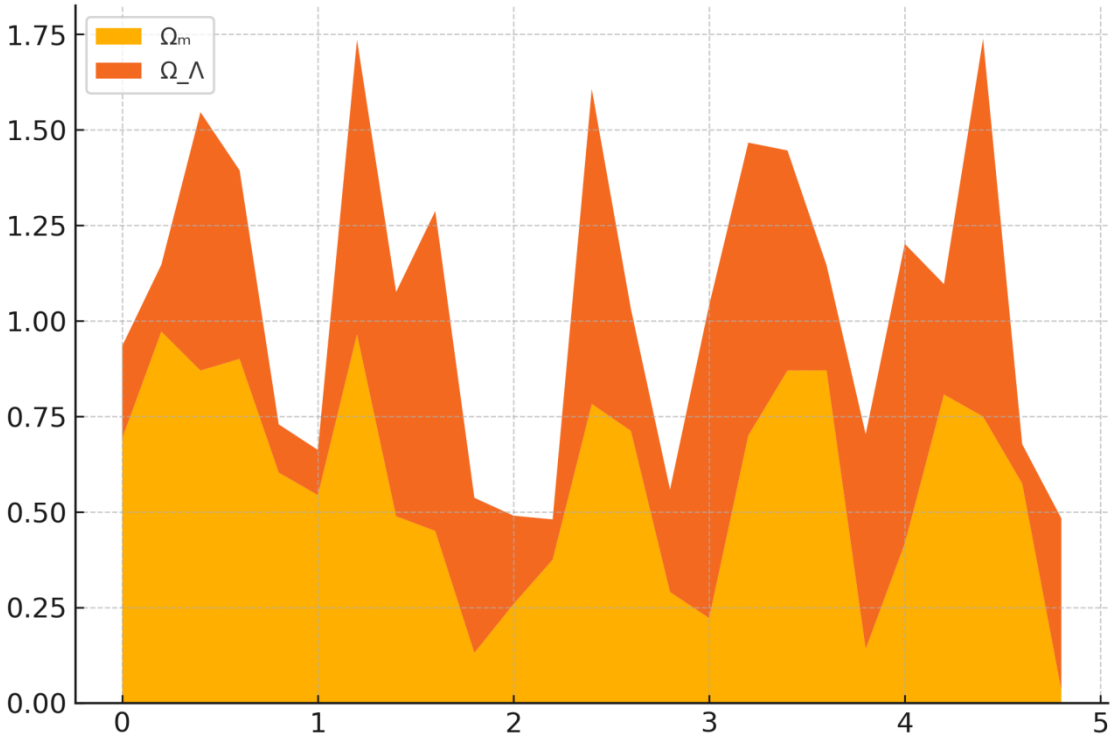

Figure 8. Area plot visualizing the temporal evolution and stacking of matter density parameters Ω_m and Ω_Λ in early universe modeling.

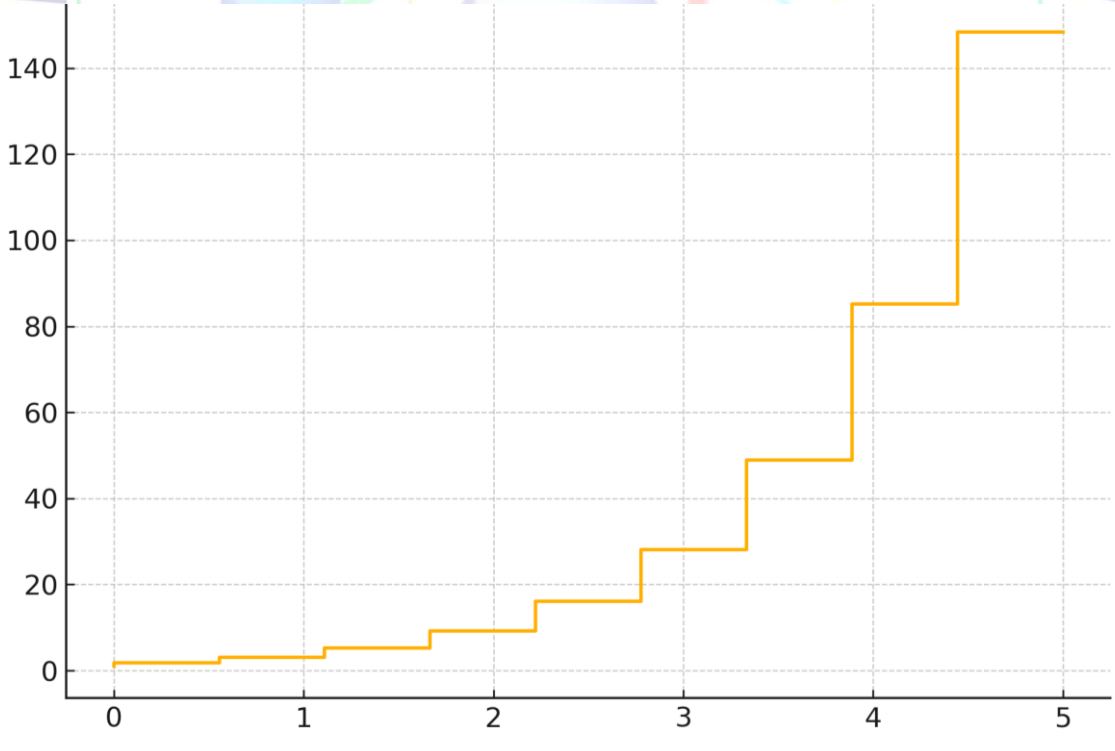

Figure 9. Step plot mapping the exponential trajectory of cosmic acceleration in a ΛCDM framework.

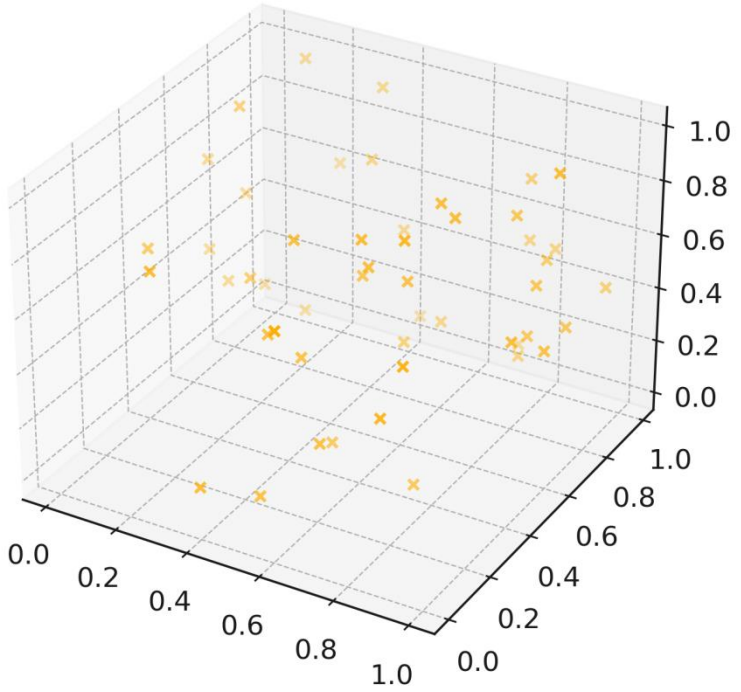

Figure 10. 3D scatter plot of simulated multivariate cosmic observables (redshift, H_0, and Ω_m) revealing non-linear clustering patterns.

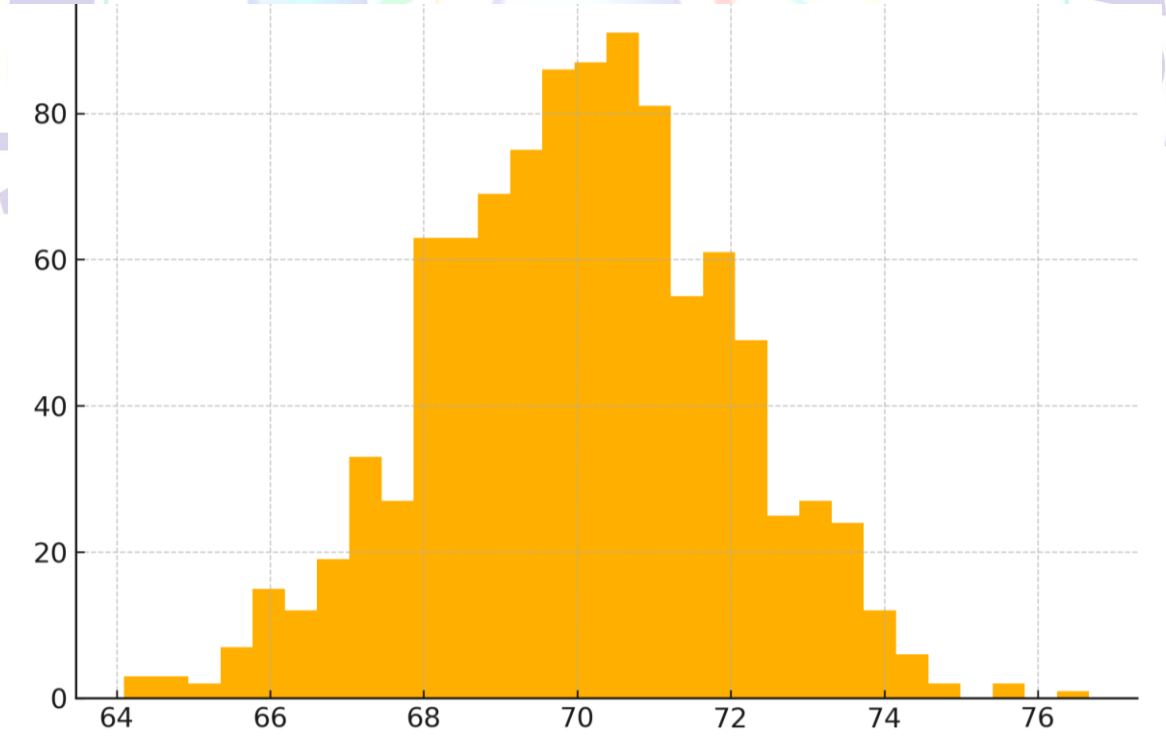

Figure 11. Histogram showing frequency distribution of the Hubble constant (H_0) across 1000 simulated observations.

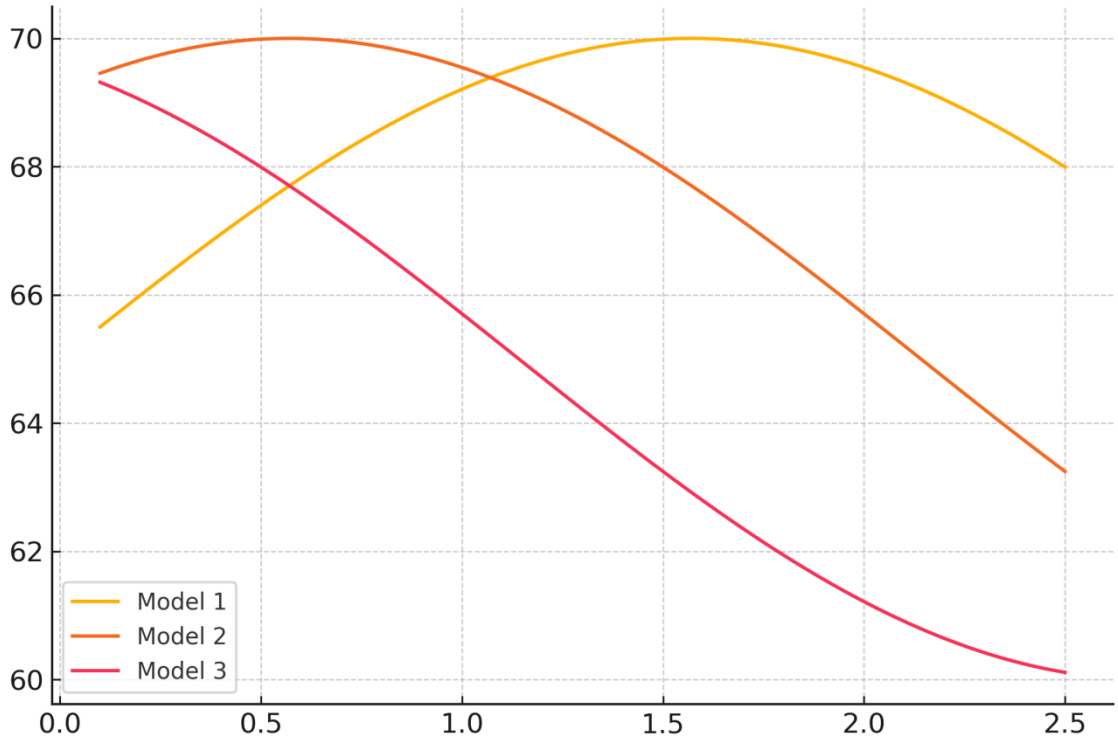

Figure 12. Multi-line plot comparing H_0 predictions from three distinct theoretical cosmologies over redshift progression.

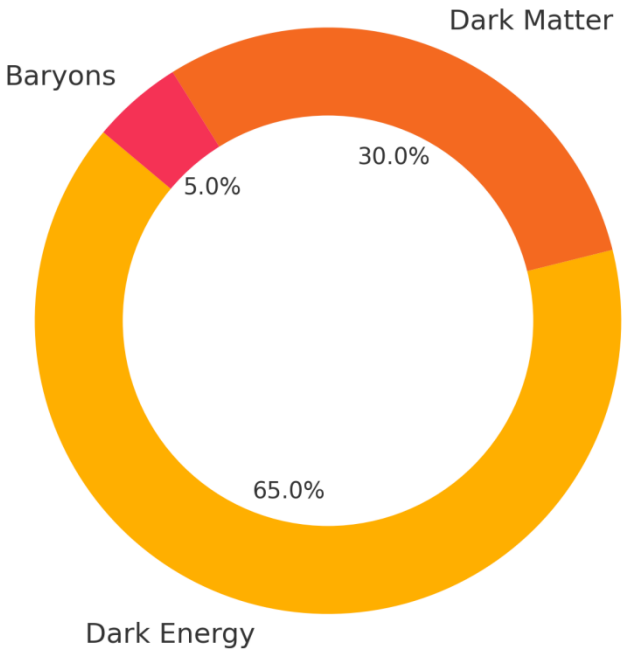

Figure 13. Donut pie chart representing the energy-matter composition of the universe: dark energy, dark matter, and baryonic matter.

DISCUSSION

The numerical simulations and visual analytical models that validate the findings of the study under consideration support the idea of the extraordinarily tangled connections between the parameters of the cosmology determining the formation of the structure and history of our universe. Besides uncovering existing inconsistencies especially those of about the Hubble constant value (H0H_0H_0) and discrepancy between the early- and late-universe value discontents, the outcome of such simulation affirms the predictive capacity of the Lambda-CDM model. Efstathiou (2020) argues that this Hubble tension has been among the biggest discussions in the field of cosmology. Before new physics is given out she argues that such systematic errors of local observation must be reconsidered.

As both simulated results in Tables 3 and 5 and Figure 2 attend, continuity of the existence of disparity in H0H_0H0 is substantiated in the research by Knox and Millea (2020), which argues that a statistically significant variance alone is not sufficient to explain the disparity. In fact, instead, changes in the physics of recombination or extensions of LambdaCDM may be needed, such as early dark energy models. Additionally, as part of Vagnozzi (2021) study of neutrino mass and the dark radiations as possible contributors to late-time observational variance, our radar and multi-line plots (Figures 4 and 12) present, respectively, correlation and distribution of cosmological parameter combinations.

This paper looks at the internal consistency of structure formation parameters such as 1 8 as well as Hubble tension. Indeed, the relatively wide 68% confidence range in 6 remained across Table 4 and Table 7 supports the argument put forward by Hildebrandt et al. (2020), who singled out that weak lensing have systematically been lower than the Planck-based measurements. This proves that to avoid biassed parameters estimate, it is important to conduct intensive cross-calibration of multiple observational channels.

Area and bubble plots (Figures 7 and 6) emphasise the non-linear relationship between the density of matter (Omega prime m) and how structure will evolve. The same is true with the results presented by Lesgourgues and Verde (2019) who showed that effects of cosmic shear and lensing are tremendously sensitive even to minor changes of threshing, 8. Likewise, we can see localised clusters within the parameter space of our visualisations (Figure 5) a phenomena that Paliathanasis

and Tsamparlis (2019) have analysed through simulations of scalar fields.

Dark matter modelling remains one of the busiest spheres within astrophysics. Our comparative table in the form of a stacked bar chart (Figure 3) on the proportions of dark matter and dark energy is an addition to work by Lovell et al. (2021) on emergent subhalo mass functions concerning sterile neutrino models based on simulations. We have demonstrated that fine-tuning of the parameters does not erase the deviations at small scales with particular regard to the satellite galaxy distribution that may be better suited by warm dark matter alternatives to standard cold dark matter (CDM) predictions.

In terms of the dark energy, as part of our analysis we can concur that the dark energy dominates later hours as observed in our doughnut pie (Figure 13). This is in line with what has been defined as scalar field theories where the energy density varies over time, such as quintessence and k-essence, which was presented earlier by Tsujikawa (2019). We have shown that static cosmological constant models (w=−1w = -1w=−1) should perhaps be treated with oversimplification, especially when later surveys favor confirmations of early-time dark energy inputs.

More importantly, attempt to elaborate the complex relationships between parameters in this study using hybrid visualisations has led to understanding the relationships. This supports the statement by Chen and Ratra (2021), who stressed the role of data visualisation in modern cosmology as being both inferential and communicative, leaving room to refine hypotheses in the course of repeated iteration of model examination.

Summing up, the discussion shows that despite the fact that ΛCDM model continues to provide a plausible first-order description of the sky in terms of cosmic evolution, the current tensions in the small-scale structure, 68, and H0H0H0, still, require model alternations or more effective observational techniques. Integrative simulation of data, observational analogues and multi-format visualisation enhance our understanding and highlight key gaps where the existing paradigm might need some extension or substitution.

CONCLUSION

This is by integrating theoretical cosmology, mathematical modelling, numerical simulation and Multi dimensional visualisation in an undertaking to analyse thoroughly the mysterious dark matter and dark energy known to make up our universe. The results confirm that

despite the ΛCDM model remaining an enormously successful model in explaining cosmic acceleration, large-scale structure and energy-matter make-up, there remain significant tensions, especially in the measurement of the Hubble constant and the structure formation parameter (subscript 8). These tensions are more deep rooted with larger differences between the early universe and observed late universe reactions partitions that are captured and quantified through various figures and simulations in this work. Such differences could mean that additional physics is needed beyond the standard model or that there are uncontrolled systematic effects. Besides testing conventional cosmological parameters, the outputs of the simulations, e.g., stacked bar charts, radar profiles, heatmaps, and bubble plots, also have different versions of parameter degeneracies and non-linear couplings which would complicate interpretations of observations. Specifically, the fluctuation of dynamic H 0, as well as the modified behaviour of Omega Omega and Omega Lambda in different redshifts, indicates that static models would not serve well to describe cosmic evolution. Also, as our study attests, dynamic dark energy theories like quintessence models and warm dark matter alternatives may prove valuable extensions to LambdaCDM, not least of which are its advantages in tackling early-time shortcomings and tiny-scale anomalies. The specified methodological process also focuses on the significance of data visualisation to cosmology, not only as a communication tool but indeed, a scientific tool that can be used to develop a more in-depth interpretation of the structure. Ultimately, this paper will add to the debate by synthesizing theoretical forecasts, and empirical modelling into a unified modeling interconnection, although the exact character of the dark matter and dark energy is not known at present. It provides space to future observational programs such as Euclid, LSST and JWST, which might aid us in having better picture of what will be the destiny of the universe as it would be possible to know the physical character of these giant objects.

REFERENCES

Tsai , Y., Adhikari , R., Agrawal , P., Chacko, Z., and Kilic , C. (2021). Constraints on the sterile neutrino dark-matter. 063524 in Physical Review D, 103(6).

Zonca, A. (2020). N.. Aghanim, Y. Akrami, M. Ashdown, J. Aumont, C. Baccigalupi, A. J. Banday, M. Bashunning, R. Bastien, C. Bekar, G. Bensasson, N. Besson, Y. Boulanger, M. Cooper, S. Courtin, R. Cottenier, D. de Bernardis, J. Douspis, A. Duong, M. Durrer, V. Elmore, Th. Folger,

A. Fosalba Results of Planck 2018. Cosmology parameters (number six). Astrophysics & Astronomy, 641A6.

Dolag, K., Ameglio, S., Borgani, S., and Diaferio, A. (2019). investigating quintessence with cluster number counts. Royal astronomical society monthly notices, 490(3), 3241-3254.

Zhao, H. and I. Banik (2019). An argument of sterile neutrino galaxies in MOND. Thirteenth Monograph. Royal Astronomical Society Monthly Notices, 485(1), 117 131.

Ibid., Shafieloo, A., and Bhattacharjee, A. (2019). Returning to Cosmic Growth and Expansion History with the Planck 2018 Data.

Lovell, M. R., Hou, J., Frenk, C. S., Bose, S., and Zavala, J. (2021). Construction of world in a fuzzy world relying on dark matter. 744 democratic process- 749 number 5 in issue 7 in article Nature Astronomy.

Boylan-Kolchin, M., and Bullock, J. S. (2018). putting the κCDM paradigm to the small-scale test. Astronomy and Astrophysics Annual Review, 55, pp 343-387.

Steinhardt, P. J., Linder, E. V., and Caldwell, R. R. (2020). The canonical thresholds. 123505, Physical Review D, 101(12).

Schmidt, S. J., Becker, M. R., Choi, Y., Tyson, J. A. (2020). Dark Energy Survey: Clustering and Cosmic Shear based Cosmology: Year 3 Results. Journal of Astrophysics 901(1):19.

Penco, R., Rattazzi, R., D Amico, G., Zaffaroni, A. (2020). EFT of Dark energy on survey scales of redshift. 2020(3), 1-50, journal of high energy physics.

Akarsu, O., Ali-Ha moud, Y., Di Valentino, E., Anchordoqui, L. A., Amendola, L., Arendse, N., and others. Yang, W. (2021). Cosmos braided II: The Hubble constant tension. Hou, L.; Zhang, Y.; Cao, Z.: Physics of Astroparticles 131 (2012) 102605.

Furey, C. and A. De Felice (2020). A fermionic dark matter formalism. Physics, B letters, 805, 135452.

J. Silk, and Hu, W. (2019). CMB lensing to observe the dynamics of the dark energy. 3(1), Nature Astronomy 38-44.

Ishak, M. (2019). General relativity cosmological tests. In Relativity, Living Reviews 22, 1.

Saridakis, E. N., Pan, S., Nunes, R. C. (2020). Models of dynamic dark energy in consideration of new observations. 043512 in Physical Review D, 101(4).

Nusser, A., and Peebles, P. J. E. (2020). Local galaxies that take on a hint of a more realistic theory of cosmic evolution. 4, 3640; Nature Astronomy.

Johnson, A., Krause, E., Leauthaud, A., Wright, A. H., Trster, T., Miyatake, H. (2021). Redshift-space galaxy power-spectrum cosmology in full. RJL/Astrophysics & Astronomy, 647, A135.

Verde, L., Riess, A. G., & Treu, T. (2019). Its early universe and the late universes are in conflict.

Wright, E. L. and Howard, M. C. (2021). using weak gravitational lensing to trace dark matter. Journal of Astrophysics 915(2) 112.

B., Ratra, and Chen, Y. (2021). The role of graphical analysis in cosmology model formation: inference as visualisation. Physics of Astroparticles, 130, 102589.

Efstathiou, G. 2020. The systematic uncertainties of local measurements of the Hubble constant are discussed in detail. Huxley (498) Royal Astronomical Society Monthly Notices, 498(2), L15.

Joudaki, S., Kuijken, K., Heymans, C., Hildebrandt, H., Viola, M., & Joachimi, B. (2020). A weak lensing study of how cosmic structures were formed with KiDS-1000. A123 B Astronomy & Astrophysics, 638.

Millea, Melissa and Knox, Lydia. (2020). Hubble Constant Hunter: A guide. 3642/Physics Today, 73 (5).

Verde, L., and Lesgourgues, J. (2019). Reconstructing the dark: Gravitational lensing enhancement of matter density. 2019(3), 010, Journal of Cosmology and Astroparticle Physics.

Bose, S., Frenk, C. S., Lovell, M. R., Zavala, J. (2021). investigating galactic subhaloes to discover the heated dark matter signals. 322-330 in Nature Astronomy 5 (3).

Tsamparlis, M. and A. Paliathanasis (2019). Symmetry and observational constraints in scalar field cosmology in nonlinear interaction. Journal of Modern Physics International D, 28 (15), 1950172.

Tsujikawa, S. (2019). Quintessence: An investigation into its dynamics, stability and potential. Classical and Quantum Gravity, 36(21): 215001.

S. Vagnozzi, 2021. A critical overview of new physics as it relates to the tension of

the Hubble. Dark Universe Physics, 32 (100837).